https://doi.org/10.5194/gmd-2020-377
Preprint. Discussion started: 8 January 2021

Geoscientific Model Development Discussions

A Permafrost Implementation in the Simple Carbon-Climate Model Hector

Dawn L. Woodard[1], Alexey N. Shiklomanov[2], Ben Kravitz[3,4], Corinne Hartin[1], and Ben Bond-Lamberty[1]

[1]Joint Global Change Research Institute, College Park, MD, USA 20740
[2]NASA Goddard Space Flight Center, Greenbelt, MD, USA 20771
[3]Department of Earth and Atmospheric Sciences, Indiana University, Bloomington, IN, USA 47405.
[4]Atmospheric Sciences and Global Change Division, Pacific Northwest National Laboratory, Richland, WA, USA 99352

Correspondence: Dawn L. Woodard (dawn.woodard@pnnl.gov)

Abstract. Permafrost, soil that remains below 0 °C for two or more years, currently stores more than a fourth of global soil carbon. A warming climate makes this carbon increasingly vulnerable to decomposition and release into the atmosphere in the form of greenhouse gases. The resulting climate feedback can be estimated using Earth system models (ESMs), but the high complexity and computational cost of these models make it challenging to use them for estimating uncertainty, exploring novel scenarios, and coupling with other models. We have added a representation of permafrost to the simple, open-source global carbon-climate model Hector, calibrated to be consistent with both historical data and 21st century ESM projections of permafrost thaw. We include permafrost as a separate land carbon pool that becomes available for decomposition into both CH_4 and CO_2 once thawed; the thaw rate is controlled by region-specific air temperature increases from a pre-industrial baseline. We found that by 2100 thawed permafrost carbon emissions increased Hector's atmospheric CO_2 concentration by 10-15% and the atmospheric CH_4 concentration by 10-20%, depending on the future scenario. This resulted in around 0.5 °C of additional warming over the 21st century. The fraction of thawed permafrost carbon available for decomposition was the most significant parameter controlling the end-of-century temperature change and atmospheric CO_2 concentration in the model and became increasingly significant over even longer timescales. The addition of permafrost in Hector provides a basis for the exploration of a suite of science questions, as Hector can be cheaply run over a wide range of parameter values to explore uncertainty and easily coupled with integrated assessment models to explore the economic consequences of warming from this feedback.

1 Introduction

Permafrost—soil that continuously remains below 0°C for at least two consecutive years—underlies an area of 22 (± 3) million km^2, roughly 17% of the Earth's exposed land surface (Gruber, 2012), and is estimated to contain 1460-1600 Pg of organic carbon (Schuur et al., 2018). Recent increases in global air temperature (Stocker et al., 2013), which are amplified at high latitudes (Pithan and Mauritsen, 2014), have resulted in widespread permafrost thaw (Romanovsky et al., 2010), and simulations from variety of climate and land surface models across a wide range of scenarios suggest that this trend will continue into the future (Koven et al., 2013; Chadburn et al., 2017).

https://doi.org/10.5194/gmd-2020-377
Preprint. Discussion started: 8 January 2021


Geoscientific Model Development Discussions

As permafrost thaws, this carbon becomes available to microbes for decomposition, resulting in the production of carbon dioxide (CO_2) and methane (CH_4) (Treat et al., 2014; Schädel et al., 2014; Schädel et al., 2016; Bond-Lamberty et al., 2016) that could lead to further warming (Koven et al., 2011; Schuur et al., 2015). Accounting for this permafrost carbon-climate feedback generally increases projections of greenhouse gas concentrations and global temperatures (Schuur et al., 2015; Burke et al., 2020) and increases estimates of the economic impact of climate change (Hope and Schaefer, 2015; Yumashev et al., 2019; Chen et al., 2019). However, the magnitude of this feedback is still highly uncertain, due to limited data availability and missing process-based understanding (Burke et al., 2020). The potential impact ranges from negligible to large, with stronger effects possible particularly over longer time horizons (Schuur et al., 2015).

Land surface models, like the Community Land Model (CLM) and JULES, use process-based representations of permafrost and can explicitly model relevant components such as soil heat flux, soil moisture, hydrology, and vegetation and can output thaw extent and depth, as well as emissions from permafrost soils (Chadburn et al., 2015; Lawrence et al., 2012). However, these high complexity models require large numbers of inputs and are computationally expensive, making it challenging to use them for uncertainty quantification.

Conversely, simple climate models such as MAGICC (Meinshausen et al., 2011) and Hector (Hartin et al., 2015) sacrifice spatiotemporal resolution and de-emphasize process realism in favor of conceptual simplicity and fast execution time. As a result they can be used to explore permafrost effects over a wide range of parameters and to analyze the relative significance of various permafrost controls. Similar models models have previously been used to explore permafrost processes such as abrupt thaw that are not yet included in Earth system models (Turetsky et al., 2020) and to understand structural and parametric uncertainty (Schneider von Deimling et al., 2015; Chadburn et al., 2017; Koven et al., 2015b). Simple climate models can also be calibrated to emulate the mean global behavior of ESMs to a high degree of accuracy (Meinshausen et al., 2011).

Here we describe the addition of permafrost thaw to the simple carbon-climate model Hector, with the goal of providing a long-term platform for addressing a suite of science questions. Hector has been used for a wide range of analyses including climate effects on hydropower (Arango-Aramburo et al., 2019), ocean acidification (Hartin et al., 2016), and global building energy use (Clarke et al., 2018), and for exploring the effects of observational constraints on estimates of climate sensitivity (Vega-Westhoff et al., 2019). Including a representation of permafrost in this model will allow for the consideration of permafrost in future such analyses with Hector, and will be particularly important to evaluating regional impacts of climate change in high latitudes.

2 Hector Model Design

Hector (Hartin et al., 2015, 2016) is an open source, object-oriented simple carbon-climate model that can emulate the global-scale behavior of more sophisticated climate models. Hector's simplicity and modular design make it easy to tweak or substantially change Hector's internal structure, while its fast computation time (1-2 seconds) allows for easier interpretation of model behavior and facilitates sensitivity and uncertainty analyses, as well as prototyping of new submodules and features. Another significant advantage of Hector is ease-of-use due to low memory requirements, ease-of-compilation, and an R interface for

https://doi.org/10.5194/gmd-2020-377
Preprint. Discussion started: 8 January 2021

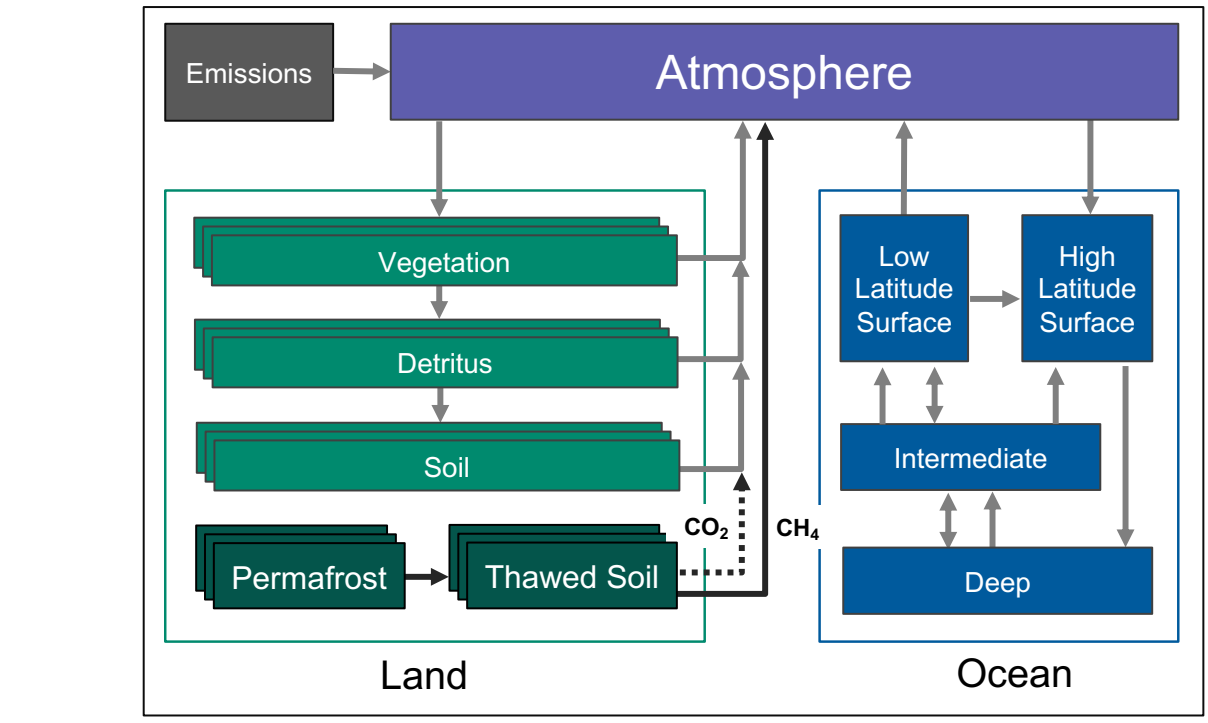

Figure 1. Hector's default carbon cycle showing fluxes (arrows) between each carbon pool. The terrestrial carbon cycle pools can be split into multiple groups, such as biomes or regions, so these are shown with multiple boxes. In darker green we show the addition of our novel permafrost representation in Hector. As carbon is exchanged in a variety of forms in Hector, the carbon flux arrows do not correspond to any particular carbon compound except where specified for land emissions. Vegetation, detritus, soil all emit CO_2, while thawed soil produces both CO_2 and CH_4 emissions.

setting inputs and parameters and retrieving model outputs. We focus here on Hector's carbon cycle as relevant to the addition of a permafrost carbon pool, but for a detailed description of the structure, components, and functionality of the base version of Hector see Hartin et al. (2015). For subsequent updates, see the Hector repository https://github.com/JGCRI/hector.

Ocean carbon in Hector is exchanged between the atmosphere and four carbon pools that model both physical circulation and chemical processes in the ocean. Carbon is taken up from the atmosphere in the high latitude surface box, which transfers some portion of this carbon to the deep ocean carbon pool. Carbon from there circulates up to the intermediate ocean layer and finally up to the high and low latitude surface pools. Carbon is then outgased back to the atmosphere from the low latitude surface pool (Figure 1).

Hector's default terrestrial carbon cycle includes three land carbon pools: vegetation, detritus and soil, which can each be separated across multiple user-defined groups (that can correspond to divisions like biomes, latitude bands, or political units), each with their own set of parameters. The vegetation pool takes up carbon from the atmosphere as net primary productivity (NPP), some of which is tranferred into the detritus pool, which can be decomposed and enter the soil carbon pool. All three

https://doi.org/10.5194/gmd-2020-377
Preprint. Discussion started: 8 January 2021


Geoscientific Model Development Discussions

land carbon pools separately emit carbon back to the atmosphere from land use change, and soil and detritus release additional carbon through decomposition-driven microbial respiration (Figure 1).

The annual change in atmospheric carbon in Hector, $\frac{dC_{atm}}{dt}$, at time t is given by:

$$\frac{\Delta C_{atm}}{dt}(t) = F_A(t) + F_{LC}(t) - F_O(t) - F_L(t) \tag{1}$$

where F_A is the flux of anthropogenic industrial and fossil fuel emissions, F_{LC} is land use change emissions, F_O is the net atmosphere-ocean carbon flux, and F_L is the land-atmosphere carbon flux. F_L is the sum of NPP and heterotrophic respiration fluxes across all user-defined groups, i:

$$F_L(t) = \sum_{i=1}^{n} \text{NPP}_i(t) - \sum_{i=1}^{n} \text{RH}_i(t) \tag{2}$$

Heterotrophic respiration for group i at time t ($RH[i,t]$) includes contributions from both soil and detritus decomposition:

$$RH[i,t] = RH_s[i,t] + RH_d[i,t] \tag{3}$$

$$RH_d[i,t] = \frac{1}{4} C_d Q_{10}[i]^{T[i,t]/10} \tag{4}$$

$$RH_s[i,t] = \frac{1}{50} C_s Q_{10}[i]^{T_{200}[i,t]/10} \tag{5}$$

where $T[i,t]$ is the change in annual mean temperature (K) since the initial model period in group i at time t (modeled as the globally averaged mean annual temperature at time t multiplied by a group-specific warming factor). Detritus and soil heterotrophic respiration are both proportional to the sizes of their respective carbon pools (C_d and C_s, both in Pg C), with a rate that increases exponentially with temperature according to a region-specific temperature sensitivity parameter (Q_{10}). Detritus respiration increases with region-specific air temperature change ($T[i,t]$), while soil respiration increases with the 200-year running mean of air temperature ($T_{200}[i,t]$), a smoothing used in Hector as a proxy for soil temperatures. This dampens the variability and produces a slower response in soil warming compared to air temperatures. Note that in Eqns. 3-5 respiration fluxes include only CO_2 emissions.

2.1 Permafrost Submodel

We added permafrost to Hector as an additional soil carbon pool that does not decompose or otherwise interact with the rest of Hector's carbon cycle until it thaws. Following previous modeling approaches, we focus on only the top 3 m of permafrost (Kessler, 2017; Koven et al., 2015b), which is also consistent with other soil carbon pools in Hector. At each time step, a temperature-controlled fraction of permafrost carbon is exchanged between the permafrost and thawed permafrost carbon pools. In the thawed permafrost pool carbon is available for decomposition into CO_2 and CH_4. Primarily carbon moves from the permafrost pool to the thawed pool as temperatures rise in the future, but refreeze of thawed carbon is also possible in scenarios where emissions reductions allow for potential cooling.

https://doi.org/10.5194/gmd-2020-377
Preprint. Discussion started: 8 January 2021


Geoscientific Model Development Discussions

For a permafrost carbon pool at time t, $C_{perm}[t]$, and a thawed permafrost carbon pool, $C_{thawed}[t]$, (both in units of Pg C), permafrost carbon in Hector is exchanged as:

$$C_{perm}[t] = C_{perm}[t-1] + \Delta C_{perm}[t] \tag{6}$$

$$C_{thawed}[t] = C_{thawed}[t-1] + \Delta C_{perm}[t] + F_{thawed-atm} \tag{7}$$

where $\Delta C_perm[t]$ is the change in the permafrost carbon pool at time t due to permafrost thaw or refreeze. Assuming a uniform permafrost carbon density, $\Delta C_{perm}[t]$ is given by:

$$\Delta C_{perm}[t] = (\Phi[t] - \Phi[t-1]) \cdot C_{perm}[t-1] \tag{8}$$

where $\Phi[t]$ is the fraction of permafrost remaining at time t.

To a first approximation, $\Phi[t]$ can be estimated as a function of mean air temperature (global or adjusted by a biome-specific warming factor). We calculate Φ at each timestep in Hector following the model reported by Kessler (2017), but we recalibrated the model to use high latitude temperatures, T_{HL}, instead of global mean surface temperatures, and we use a lognormal cumulative distribution function instead of a linear model in order to allow for slower thaw in deeper permafrost and to bound the output by zero and one.

$$\Phi[t] = 1 - \text{NCDF}(\log(\Delta T_{HL})|\mu, \sigma) \tag{9}$$

where $NCDF$ is the normal cumulative distribution function and μ and σ are the mean and standard deviation of the lognormal distribution. These two parameters control the frozen fraction of permafrost as a function of temperature and can be interpreted as follows: e^{μ} is the temperature at which 50% of the permafrost is thawed, while σ controls how sudden the thaw is around the mean relative to lower and higher temperatures. Technically, permafrost area could increase in the case of cooling temperatures, and therefore the area fraction could be greater than one. However, because even the most aggressive climate action scenarios show future temperatures that stabilize above early 21st century temperatures, we assume that permafrost area will never grow more than the starting value.

2.1.1 Permafrost Carbon Emissions

Even after thaw, only a fraction of permafrost carbon is available to decompose, while the remainder is inert. This non-labile fraction of carbon, f_{static}, is removed from the thawed permafrost carbon pool at each time step before decomposition. Of the remaining labile fraction, most decomposes aerobically to CO_2 from microbial respiration, while a small fraction generates CH_4 emissions from anaerobic respiration. Heterotrophic respiration emissions from Hector's thawed permafrost carbon pool are partitioned between CO_2 and CH_4 based on a CH_4 respiration fraction, f_{CH4}.

With the addition of permafrost in Hector, the total heterotrophic respiration flux of CO_2 ($RH[i,t]$) for biome i at time t is the sum of heterotrophic respiration in detritus (RH_d), soil (RH_s), and thawed permafrost (RH_{pf}):

$$RH[i,t] = RH_s[i,t] + RH_d[i,t] + RH_{pf}[i,t] \tag{10}$$

https://doi.org/10.5194/gmd-2020-377
Preprint. Discussion started: 8 January 2021

Geoscientific Model Development Discussions
Open Access
EGU

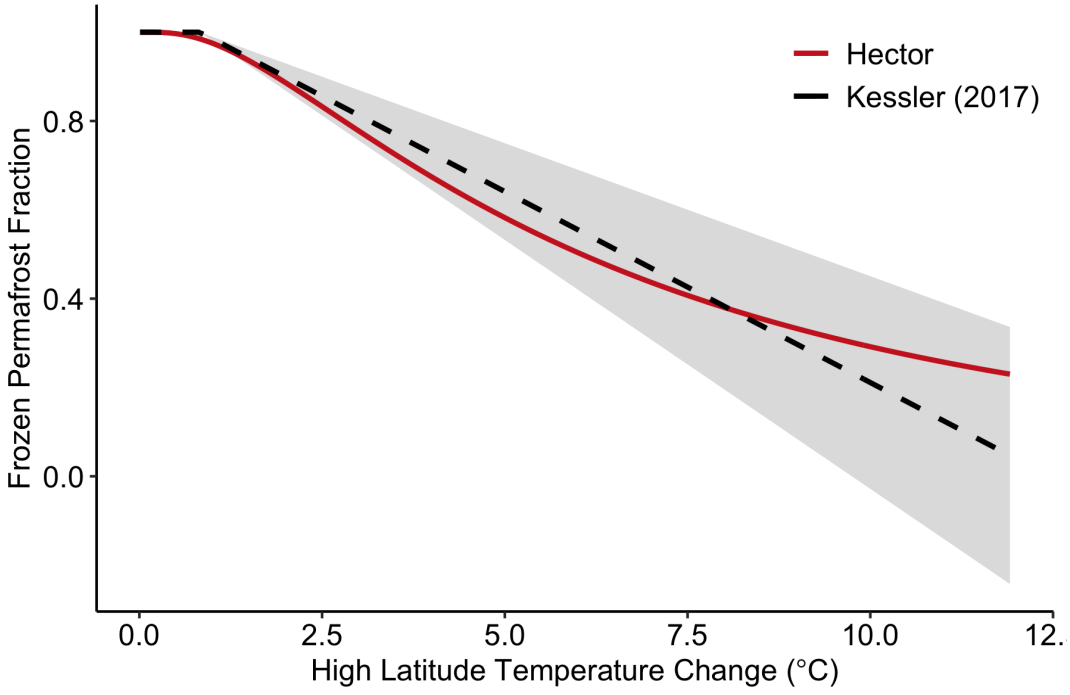

Figure 2. Lognormal permafrost-temperature relationship (red) in Hector with $\mu = 1.80$ (e^{μ}=6.05) and $\sigma = 0.917$, compared with our high latitude temperature-adjusted form of the linear model in Kessler (2017) (black). The shaded area shows the upper and lower bounds given by plus or minus one standard deviation from our adjusted version of the best estimate model in Kessler.

The thawed permafrost CO_2 repiration flux, RH_{pf}, is proportional to the size of the thawed pool, C_{thawed}, based on the non-labile fraction of carbon in that pool, f_{static}, and to the fraction of emissions released as CH_4, and increases exponentially with the 200-year running mean of temperature, following the formulation from Hector's default soil pool.

$$RH_{pf}[i,t] = (1 - f_{static}) \cdot (1 - f_{CH4}) \cdot C_{thawed} \cdot Q_{10}[i]^{T_{200}[i,t]/10} \tag{11}$$

The CH_4 respiration flux from thawed permafrost is estimated similarly, but is added to natural CH_4 emissions in Hector, which are prescribed at 300 Tg year^{-1} (Hartin et al., 2015) to affect atmospheric CH_4 concentrations.

$$RH_{CH4}[i,t] = (1 - f_{static}) \cdot (f_{CH4}) \cdot C_{thawed} \cdot Q_{10}[i]^{T_{200}[i,t]/10} \tag{12}$$

While there are other processes occurring (see Discussion) these are thought to be the major processes controlling decadal permafrost dynamics (Schuur et al., 2015).

2.2 Configuration and Tuning

To run Hector with permafrost we separated the land component of the model into permafrost and non-permafrost regions (groups). In the permafrost region all parameters were set to the values given in Table 1, and we allocated 10% of the initial

https://doi.org/10.5194/gmd-2020-377
Preprint. Discussion started: 8 January 2021

Geoscientific Model Development Discussions

global vegetation carbon (equivalent to 55 Pg C McGuire et al. 2018), 2% of the initial detritus carbon (1 Pg C), and 13% of the global soil carbon (equivalent to 308 Pg C, following Hugelius et al. 2014) to this region. Initial permafrost carbon in Hector was set to 825 (± 150) Pg C based on the 727 Pg C estimate for near-surface (<3 m depth) permafrost by Hugelius et al. (2014) and scaled up based on historical thaw in the model so that the resulting modern value is close to 727 Pg C. We did not use the full 1035 Pg C reported in Hugelius et al. (2014) here, as this includes both frozen and non-frozen soil, and we instead allocated the remaining 308 Pg C to non-permafrost soil in the permafrost region.

Table 1. Hector configuration of permafrost-related parameters and initial values based on literature review. Ranges shown are used for the sensitivity analysis. $C_{perm}(t=0)$ was estimated by scaling up 727 Pg C (Hugelius et al., 2014) based on the fraction of permafrost lost by 2010. The soil and vegetation carbon initial values refer to non-permafrost carbon in the permafrost region, and μ and σ are tuned parameters estimated by optimizing the model against results from Koven et al. (2013).

Parameter	Hector Nomenclature	Value	Estimated Range	Reference	Description
μ	`pf_mu`	1.80	1.80-2.13	tuned to Kessler (2017)	Permafrost-thaw parameter
σ	`pf_sigma`	0.917	0.90-1.03	tuned to Kessler (2017)	Permafrost-thaw parameter
f_{static}	`fpf_static`	0.40	0.13-0.60	Burke et al. (2012, 2013)	Non-labile permafrost fraction
$C_{perm}(t=0)$	`permafrost_c`	825 Pg C	675-975 Pg C	Hugelius et al. (2014)	Initial permafrost carbon
$C_{soil}(t=0)$	`soil_c`	308 Pg C	—	Hugelius et al. (2014)	Initial non-permafrost soil in the permafrost region
$C_{veg}(t=0)$	`veg_c`	55 Pg C	—	McGuire et al. (2018)	Initial vegetation stock in the permafrost region
wf	`warmingfactor`	2.0	1.75-2.25	Pörtner et al. (2019)	High-latitude warming factor
f_{RH_CH4}	`rh_ch4_frac`	0.023	0.01-0.03	Schuur et al. (2013); Schneider von Deimling et al. (2015)	Fraction of thawed permafrost carbon decomposed as CH_4

We also amplified warming in the permafrost region as a constant multiple of global mean temperatures in Hector, to account for increased rates of warming at high latitudes. We set this warming factor to 2.0 (Pörtner et al., 2019).

We used the upper and lower bounds (± one standard error from the best estimate in Kessler) to recalibrate the model in Kessler (2017) to high latitude temperatures and then fitted our lognormal distribution parameters μ and σ to the upper and lower bounds of this adjusted model version. We then used these parameter ranges to tune the permafrost module against CMIP5 multi-model mean output, using the "L-BFGS-B" method from the `optim` function in the R `stats` package. We tuned based on the fraction of permafrost lost over the historical period, and from 2005-2100 in RCP4.5 and RCP8.5 as reported in Koven et al. (2013). We were able tune to closely match future projections, but in order to keep μ and σ within the bounds from Kessler (2017), we sacrificed some accuracy in historical permafrost change, underestimating this loss by around 35% in our best model (Koven et al. 2015b, Table 2). The final tuned value of σ that we used as our default baseline in this analysis was

https://doi.org/10.5194/gmd-2020-377
Preprint. Discussion started: 8 January 2021

Geoscientific Model Development Discussions

Table 2. Values used for tuning Hector's parameters (column 4) compared against final values in Hector after tuning (column 5). The modern permafrost value in Hector was taken from the year 2010. Koven et al. (2013) values are from the top 50% of CMIP5 models reported in that analysis based on accuracy of modern permafrost area. As we do not consider deep permafrost in the model, values for the remaining permafrost area in each time period only include permafrost at less than 3 m depth.

Scenario	Source	Variable	Value	Hector
—	Hugelius et al. (2014)	Modern Permafrost Carbon 0-3m (Pg C)	727	767.0
RCP4.5	Koven et al. (2013)	Remaining Permafrost Area 1850-2005 (%)	84	89.6
RCP4.5	Koven et al. (2013)	Remaining Permafrost Area 2005-2100 (%)	58	58.6
RCP8.5	Koven et al. (2013)	Remaining Permafrost Area 2005-2100 (%)	29	33.3

0.917, while the tuned value of μ was 1.80, which is at the lowest end of the available range. To give a more intuitive sense of this number, e^{μ}, or 6°C, corresponds to the high latitude temperature difference since pre-industrial at which only 50% of all shallow permafrost will remain.

Estimates of the fraction of inert carbon (not vulnerable to decomposition) vary widely but we use a mean of 0.40 (0.13-0.60) based on estimates by Burke et al. (2012, 2013). Estimates from Schädel et al. (2014) found this fraction to be even higher, close to 70% of permafrost carbon. The partitioning between CH_4 and CO_2 emissions from thawed permafrost carbon systems depends on soil drainage and anoxia and is highly uncertain (Knoblauch et al., 2018; Schädel et al., 2016; Schuur et al., 2013). We set the share of CH_4 to be 2.3% of total emissions, from (Schuur et al., 2013), although a more recent meta-analysis indicates that it could be around 4.3% (Schädel et al., 2016).

2.3 Evaluation

We ran Hector with and without permafrost feedbacks using forcings from each of four Representative Concentration Pathways (RCPs), RCP2.6, RCP4.5, RCP6.0, and RCP8.5 (Moss et al., 2010). We chose these scenarios to broadly demonstrate the impacts of a wide range of future climate conditions on permafrost thaw and permafrost-driven carbon emissions and for ease of comparison with other results. The only difference between our model runs with and without permafrost feedbacks is that the baseline (no-permafrost) configuration of Hector is initialized with $C_{perm}(t = 0)$ set to 0 to turn off permafrost feedbacks. Our analysis focused on the 21st century, but we also show some longer term effects of permafrost out to 2300. Hector has not been calibrated over this period, however, and these findings should be taken as provisional. We also ran the model with and without active CH_4 emissions to estimate the separate contributions of permafrost-driven CO_2 and CH_4 emissions to the permafrost climate feedback.

Given that much uncertainty remains surrounding permafrost controls, we evaluated the sensitivity of three key climate and carbon cycle outcomes (temperature anomalies and atmospheric CO_2 and CH_4 concentrations) to changes in each of the permafrost-specific parameters in Hector across their estimated ranges from the literature (Table 1). The parameters we include are the permafrost thaw parameters, μ and σ; the initial size of the shallow permafrost pool available for thaw ($C_{perm}(t = 0)$);

https://doi.org/10.5194/gmd-2020-377
Preprint. Discussion started: 8 January 2021


Geoscientific Model Development Discussions

the fraction of thawed permafrost that is not available for decomposition (f_{static}); and the fraction of thawed permafrost carbon emissions that decomposes to CH_4 (f_{RH_CH4}). From these parameters we generated priors by sampling from normal distributions centered on the default values of each parameter from Table 1. We then ran Hector with 500 parameter sets drawn from the prior distributions. Based on the effects on temperature and atmospheric CO_2 and CH_4 in 2100 in each of these model runs, we estimated the coefficient of variation, elasticity, prediction variance and partial variance of each paramter. We follow the approach of LeBauer et al. (2013), except that while LeBauer et al. (2013) fit a cubic spline interpolation through each parameter-output combination, we used a multivariate generalized additive model regression. This allowed us to calculate partial derivatives across the median of each parameter, making for simpler computation and easier interpretation.

3 Results

This Hector implementation of permafrost thaw and loss reproduced the magnitude and general temporal trajectory of globally averaged permafrost thaw simulated by ESMs and by simpler permafrost thaw models (Koven et al., 2015a; Burke et al., 2017; Schuur et al., 2015; McGuire et al., 2018). In RCP 4.5, 6.0, and 8.5, permafrost losses reached 300-400 Pg C by 2100 and mostly leveled off after this point (Figure 3a). RCP2.6 is unique in that strong emissions mitigation in this scenario leads to cooling temperatures, which allowed for permafrost recovery (i.e., re-freeze of carbon from the thawed permafrost pool) to begin by the end of the century in Hector. In all scenarios, the thawed permafrost carbon pool increased to a peak around mid-century, at which point losses to CH_4 and CO_2 from heterotrophic respiration began to outpace the carbon inputs from new permafrost thaw. Over longer timescales, carbon stocks of thawed permafrost carbon dropped to zero.

The influence of permafrost on the net land-atmosphere carbon flux in Hector was strongest while respiration emissions from permafrost thaw were at their peak, around mid-century, resulting in a peak increase of up to 3 Pg C yr^{-1}. This almost entirely offset the existing land sink, such that the net land-atmosphere flux in our permafrost run remained near zero through 2100 in all scenarios but RCP8.5. This influence of permafrost reduced almost to zero by 2300 (Figure 3c) since warming, and thus permafrost thaw, flattened soon after the end of the 21st century in all scenarios. On the other hand, the changes in the non-permafrost land-atmosphere flux due to permafrost in Hector increased until the end of the century, after which they declined and resulted in net losses by 2300, driven by higher temperatures and thus increasing losses of soil carbon from heterotrophic respiration.

We found that including CH_4 emissions in the model, set to the default fraction of 2.3% of emissions from thawed permafrost carbon, increased the strength of the effect of the permafrost feedback on global mean temperatures by 25%, adding around 0.1°C of warming by 2100 in RCP4.5. The relatively short lifetime of CH_4 in the atmosphere (estimated as 9.1 years by Stocker et al., 2013) means that the effects of the permafrost carbon feedback on atmospheric CH_4 concentrations across the RCPs followed a similar trajectory to that of thawed permafrost carbon, though lagged by a few years. As the thawed permafrost carbon pool shrank and CH_4 emissions from this pool declined, permafrost-driven changes in atmospheric CH_4 also dropped off, falling to zero by 2300 (Figure 3b,d).

https://doi.org/10.5194/gmd-2020-377
Preprint. Discussion started: 8 January 2021

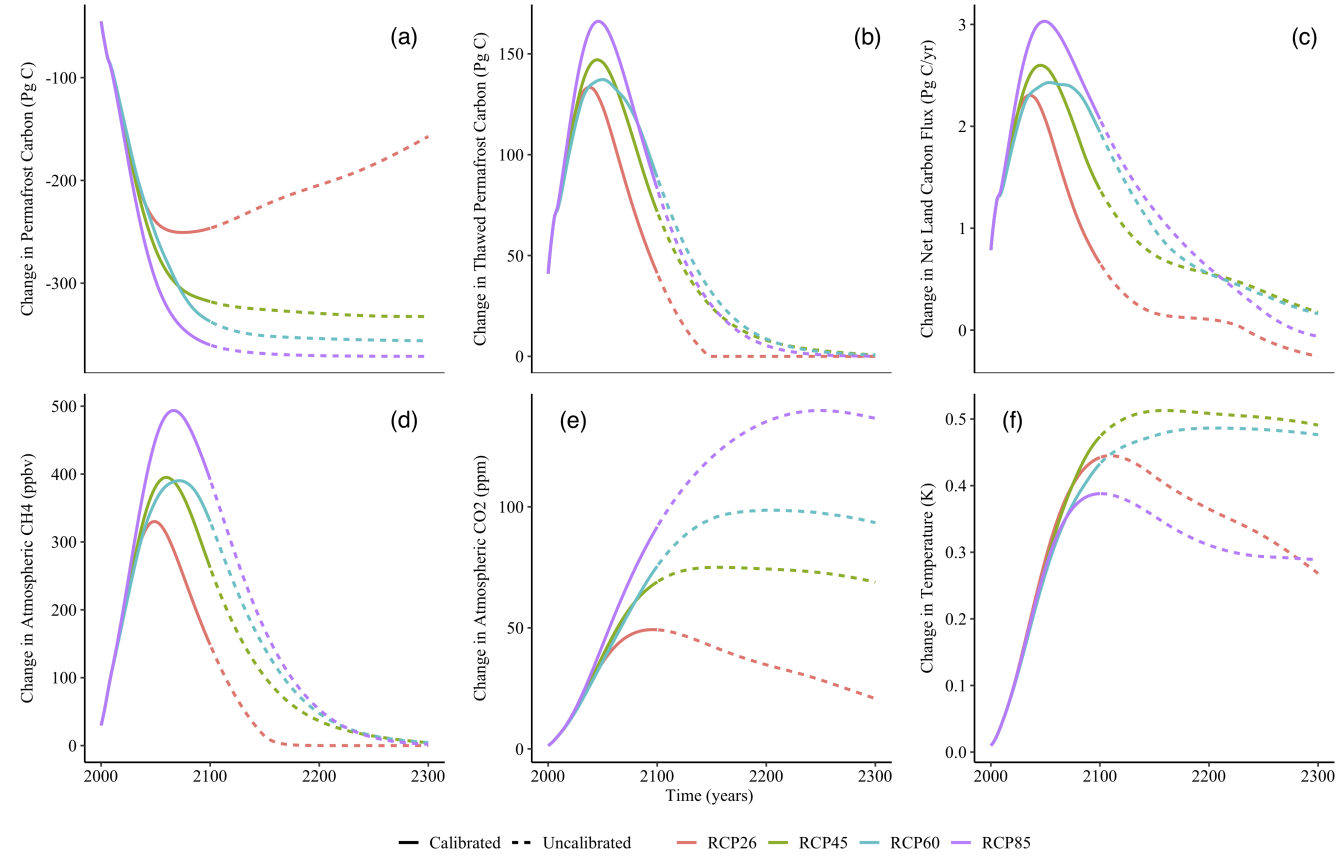

Figure 3. Effect on key climate and carbon outputs of including permafrost in Hector, shown as the difference between a model run with and without active permafrost processes under the default model configuration across RCP2.6, RCP4.5, RCP6.0, and RCP8.5. Results are shown through 2100 (solid lines) as the calibrated period of Hector, but are extended to 2300 (dashed lines) to illustrate potential long term dynamics. The net land carbon flux is the sum of the land-atmosphere carbon fluxes: soil, detritus, and thawed permafrost respiration fluxes of CO_2, thawed permafrost CH_4 emissions, land use change, and net primary productivity, and is defined as positive into the atmosphere.

The much longer lifetime of atmospheric CO_2 (300 to 1000 years; Stocker et al. 2013), meant that the permafrost-driven increases remained over the entire model run time, long after actual permafrost emissions dropped to zero. Permafrost emissions also drove a steady increase in temperature over the 21st century, which leveled off as emissions declined. Consistent with previous findings (e.g., Burke et al., 2017; MacDougall et al., 2012, 2013), the influence of permafrost on temperature was less significant in higher RCPs (declining from a 30% increase in RCP2.6 to a 9% increase in RCP8.5 at 2100) (Table 3). This meant that although total temperature change in Hector over the 21st century was highest in RCP8.5, the change in temperature due to permafrost was lowest in this scenario compared to the other RCPs (Figure 3f).

https://doi.org/10.5194/gmd-2020-377
Preprint. Discussion started: 8 January 2021

Geoscientific Model Development Discussions

Table 3. Permafrost results across all RCP scenarios at 2100 for several key carbon and climate outputs. All results are global and summed across permafrost and non-permafrost regions. The 'total' columns are generated by running Hector with the configuration in Table 1, while the 'change' columns give the percent change from a baseline model run without active permafrost.

	Scenario							
	RCP26		RCP45		RCP60		RCP85	
Output	Total	Change (%)	Total	Change (%)	Total	Change (%)	Total	Change (%)
Remaining Permafrost Carbon (Pg C)	578.5	-29.9	507.1	-38.5	487.7	-40.9	464.9	-43.7
Net Permafrost CO_2 Emissions (Pg C)	196.8	0	237.4	0	240	0	267.8	0
Atmospheric CO_2 (ppm)	431.2	13.7	571.5	14.6	722	12.4	982.9	11.1
Net Permafrost CH_4 Emissions (Pg C)	4.6	0	5.6	0	5.7	0	6.3	0
Atmospheric CH_4 (ppbv)	1335.6	12.5	1924.5	15.8	2117.9	18.4	4683.9	9.1
Non-Permafrost Soil Carbon (Pg C)	1873.6	0.7	1934.7	0.5	1968.6	0.3	1979.1	-0.1
Detritus Carbon (Pg C)	61.6	2.7	64.8	2.3	67.3	1.6	69.6	0.9
Vegetation Carbon (Pg C)	580.4	3.4	617.7	3.2	637.9	2.8	675.2	2.5
Temperature Anomaly (K)	2	29.5	3	19.4	3.6	14.3	5.1	8.7

3.1 Permafrost effects on carbon pools

Across the four RCP scenarios, between 133 and 283 Pg C (in RCP2.6 and RCP8.5, respectively) of permafrost carbon was thawed by 2100 when all permafrost parameters were set to their default values in Table 1. Between 2000 and 2100 this newly available carbon moved from the thawed pool to the atmosphere and then into the ocean and non-permafrost land carbon pools (Figure 4). In RCP8.5 69% (197 Pg C) was decomposed and emitted to the atmosphere as CO_2 and CH_4 by the end of the century. Of that 69%, around 140 Pg C remained in the atmosphere, while 30 Pg C was taken up by the ocean and 10 Pg C each were taken up by the non-permafrost soil and vegetation pools. The effect on the detritus pool was less than 1 Pg C. Over longer timescales, the fraction of thawed permafrost carbon emitted to the atmosphere through respiration grew to nearly 100% by 2300, and a larger fraction (close to a quarter) of that respired permafrost carbon was taken up by the ocean from the atmosphere. The higher temperatures also drove net losses in soil carbon by 2300 relative to a model run without permafrost (Figure 4).

While scenarios with lower radiative forcing thawed less permafrost carbon overall, a higher fraction of that carbon ended up released into the atmosphere by the end of the century (86% in RCP2.6). Relatively more of this carbon was also taken up by the ocean in this scenario (25% by 2100 and over 90% by 2300) thanks to lower mean global temperatures increasing the solubility of CO_2 in seawater and reducing stratification, while only 42% (56 Pg C) remained in the atmosphere by 2100 (Figure 4).

https://doi.org/10.5194/gmd-2020-377
Preprint. Discussion started: 8 January 2021

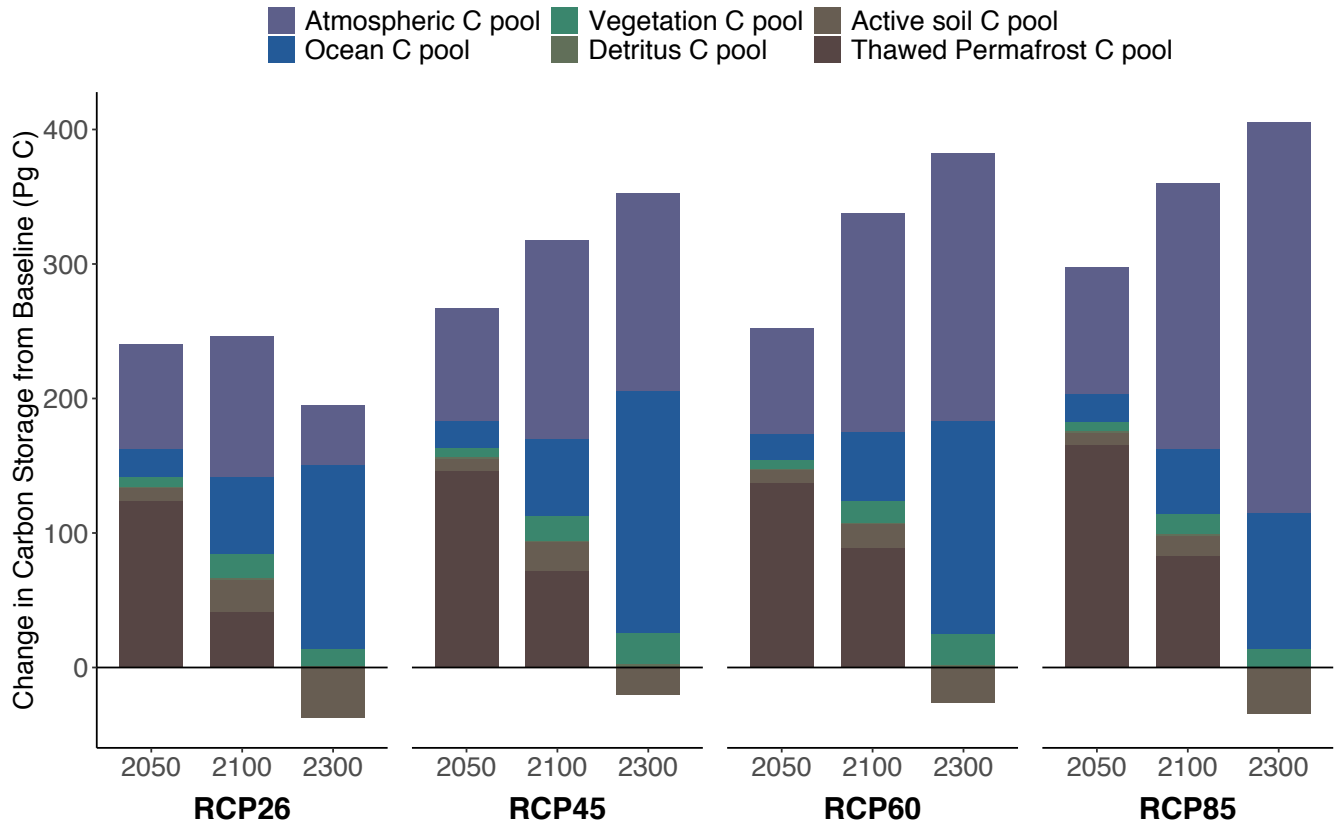

Figure 4. Changes in carbon stocks in a permafrost-active model run compared to a run without permafrost at 2050, 2100, and 2300 across all RCPs. The sum of each bar is the total carbon lost from the permafrost pool by that year in each RCP. Results for 2300 should be taken as provisional since Hector is not calibrated over this period. While more carbon moves from the thawed pool into the atmosphere, and then into the ocean across the three periods shown, a relatively larger fraction of carbon remains in the atmosphere in higher warming scenarios.

3.2 Sensitivity of Temperature Effects to Permafrost Parameters

Based on the effects on end-of-century temperature change and atmopsheric CO_2 and CH_4 concentrations, we found that the most significant permafrost control in Hector was the non-labile fraction. This accounted for 30-45% of the variance across all three outcomes (Figure 5), followed by the initial permafrost pool size (17-22% of the variance). The effect of the permafrost thaw mean parameter showed a wider range across the outcomes, responsible for only 10% of the atmospheric CH_4 variance, and 23% of atmospheric CO_2. Similarly, adjusting the permafrost thaw standard deviation also had a much smaller effect on the variance of atmospheric CH_4 (3%) and a larger effect on atmospheric CO_2 and temperature (11 and 13%, respectively). Atmospheric CH_4 concentrations in 2100 were most affected by the CH_4 fraction parameter, while this had no significant effect on atmospheric CO_2 and only a small effect on temperature.

https://doi.org/10.5194/gmd-2020-377
Preprint. Discussion started: 8 January 2021

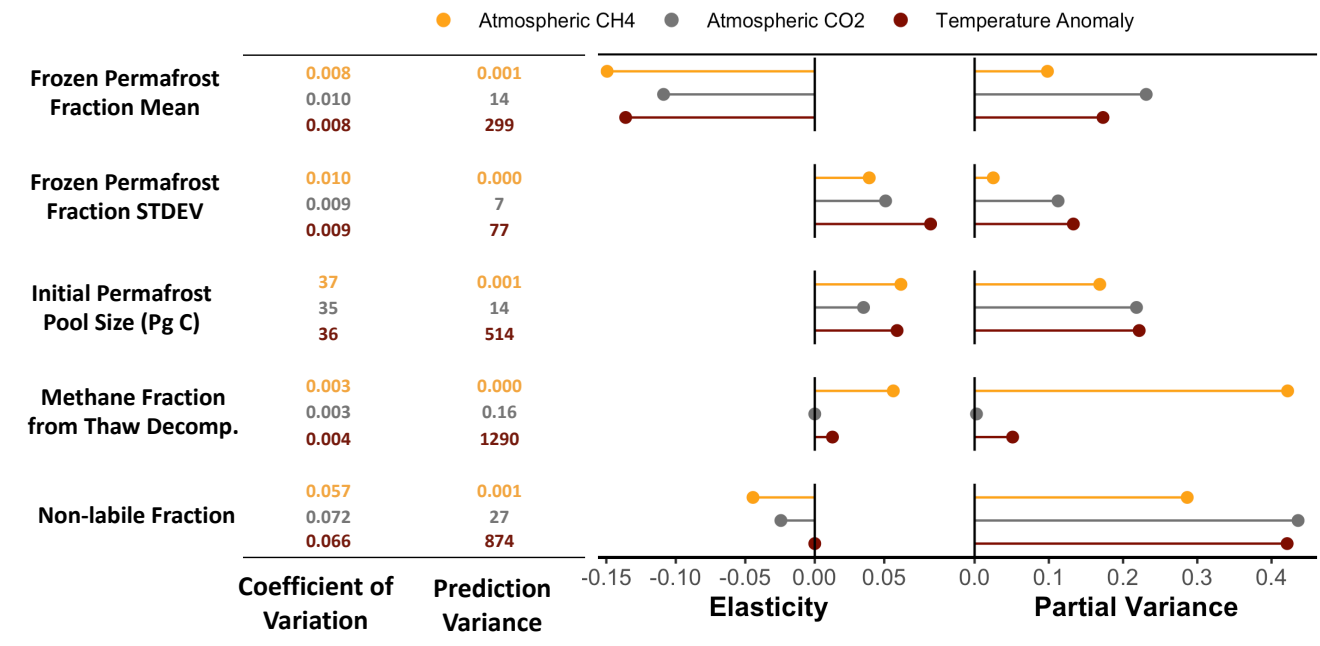

Figure 5. Sensitivity analysis of the effect of key permafrost controls on end-of-the-century atmospheric CH_4 (orange) and CO_2 (grey) concentrations as well as temperature anomalies (dark red), following LeBauer et al. (2013) and forced with RCP4.5 emissions. The coefficient of variation is the ratio between the input parameter mean and variance and reflects the parameter's relative uncertainty, elasticity is the normalized sensitivity of the model to a change in a particular parameter, the prediction variance is the variance in the model output, and finally the partial variance, or the fraction of variance in the model output that is explained by the given parameter, integrates the elasticity and prediction variance to give the overall sensitivity of the model to each parameter.

Over longer timescales out to 2300 the influence of the non-labile pool size was even stronger, while the effect of the thaw parameter σ and the CH_4 partitioning dropped to nearly zero. The negligible influence of CH_4 over longer timescales can be expected given that all carbon emissions from thawed permafrost carbon have dropped to zero by 2300 and the much shorter lifetime of CH_4 in the atmosphere compared to CO_2 means that the effect fades soon after emissions drop off.

4 Discussion and Conclusions

Including permafrost in Hector significantly increased end-of-century atmospheric CO_2 and warming, and had a shorter-term influence on atmospheric CH_4 and the land-atmosphere flux. The parameter with the most significant effects on these outcomes was the fraction of permafrost available for decomposition, or the non-labile fraction. This suggests that future research constraining this parameter may be important for reducing uncertainty in permafrost estimations moving forwards. However,

https://doi.org/10.5194/gmd-2020-377
Preprint. Discussion started: 8 January 2021


Geoscientific Model Development Discussions

given the simplicity of the permafrost represenation in Hector, the relevance of this parameter might change with a model that uses more detailed physically-based representations of the processes involved.

4.1 Model Limitations

While we attempted to use reasonable values for our model parameters and calibrated Hector to emulate the behavior of permafrost thaw in global climate models, these results should be taken as demonstrative of this model's capabilities, rather than conclusive projections, as model parameter values can be adjusted as needed to reflect the latest understanding of permafrost characteristics, and this was not our focus here. What is more important is to acknowlege the permafrost dynamics that are not captured in this model's structure.

Hector's permafrost module parameterizes gradual permafrost thaw, following previous development on simple climate models (Kessler, 2017), but leaves off consideration of abrupt thaw, which has been found to be a potentially significant contributor to future permafrost emissions (Turetsky et al., 2020), increasing the overall permafrost soil carbon emissions by 125-190% above that from gradual thaw according to a recent analysis (Anthony et al., 2018). Abrupt thaw is also missing from current Earth system models, so our tuning to these models would not account for this mechanism, and it may mean that Hector is somewhat underestimating the permafrost carbon feedback.

Hector's permafrost module also only accounts for carbon stored in the top three meters of soil, as this shallow permafrost is the most vulnerable to both thaw and decomposition (Kessler, 2017). However, analysis accounting for abrupt thaw found higher contributions from deep carbon when including these abrupt thaw processes (Schneider von Deimling et al., 2015). Previous modeling results have found that a mean of around 2 Pg C may be emitted over the next century from this deeper permafrost (Koven et al., 2015b), or an additional 3% of total permafrost-driven carbon emissions over that time period, but this study also neglected abrupt thaw processes. There may also be a larger contribution from this pool over longer term results since warming would have more time to reach these deposits, although warming in Hector levels off beyond the end of the century.

We additionally assume all thawed permafrost carbon decomposes at the same rate as soil carbon in Hector, though previous studies have drawn distinctions between rapid (residence time of <1 yr) and more slowly decaying pools (residence time of 6-9 years) (Schädel et al., 2014). This implies that permafrost decomposition may occur more slowly than is represented by Hector and thus emissions from thawed permafrost may continue longer into the 22nd century or beyond.

Thawing permafrost can affect geometry and drainage patterns of the landscape, including creating thaw lakes which are persistent sources of both CH_4 and CO_2 (Vonk et al., 2015; Matveev et al., 2016). Hector does not include hydrological processes that could account for this effect, and this additional consequence of permafrost thaw on emissions would not have been captured through tuning to CMIP5 models because we only tuned Hector against the fraction of permafrost thaw in each. While we found that permafrost emissions from Hector's thawed pool quickly dropped to zero as the thawed pool decomposed, the model is missing this longer-term affect of permafrost thaw on CH_4 and CO_2 emissions in the region.

The absence of hydrological processes in Hector also means the model misses interactions between permafrost thaw and soil moisture. Soil moisture has been found to play a critical role in the rate of release of thawed permafrost carbon, as drier

https://doi.org/10.5194/gmd-2020-377
Preprint. Discussion started: 8 January 2021


Geoscientific Model Development Discussions

soils release carbon much faster than wetter soils (Elberling et al., 2013). Thawing permafrost itself impacts soil moisture, although predicting these effects is difficult (Wickland et al., 2006). Moisture also affects the balance of aerobic and anaerobic decomposition, determining the ratio of CO_2 to CH_4 release (Turetsky et al., 2002). For example, Lawrence et al. (2015) found that permafrost thaw increased soil drying, reducing the CH_4 fraction of permafrost emissions to the extent that the global warming potential of emissions from the permafrost region was reduced by 50%. Projections of drying soils due to permafrost thaw are also supported by the analysis in Andresen et al. (2020).

While other mechanisms are included in ESMs and some of their effects on permafrost thaw can be implicitly captured through calibration, not explicitly modeling these effects can still impact temporal dynamics and the relative strength of particular outcomes. A key difference between Hector and ESMs is spatial representation. While ESMs are spatially explicit, Hector is primarily global, although with separate calculations for land biomes or other subdivisions. In the case of the results shown here, only a single permafrost "biome" was used; this combines high latitude and high elevation permafrost, although in reality these may be differently affected by climate. Future analyses with this model may choose to further sub-divide the permafrost "biome" into more specific regions or categories to better address these different dynamics.

We also made the simplifying assumption that thawed permafrost carbon does not interact with the vegetation or detritus pools, and that newly thawed permafrost carbon does not affect the potential size of the vegetation and detritus pools in the permafrost region. This means our results exclude any potential changes in plant productivity as a result of permafrost thaw, though the sign of these effects is highly uncertain (Frost and Epstein, 2014).

Finally, we do not include any insulating effect from snow and vegetation, which can protect permafrost from warmer air temperatures (Shur and Jorgenson, 2007). However, this effect may be small on the global scale, as including such protected permafrost was not found to substantially alter the amount of permafrost thaw over the next century of warming according to a 2017 analysis by Chadburn et al..

Of these limitations, we consider the most significant and likely influential on the magnitude of our results to be the lack of abrupt thaw processes, including the effects of abrupt thaw on deeper permafrost carbon. Results from Anthony et al. (2018) suggest our model may be underestimating the permafrost carbon feedback by as much as 20-50%, though there are still only limited estimates of these effects in the literature. The other significant effect on permafrost emissions estimates in Hector is the lack of hydrological processes, which would potentially generate longer term increases in emissions from permafrost thaw due to lake formation. Other mechanisms affecting rates of permafrost thaw are included in CMIP models and thus we expect to have captured the net end-of-century effects of these mechanisms through tuning to CMIP5 outputs.

4.2 Comparison to Previous Work

While our permafrost model is necessarily limited in complexity by Hector's structure and by the need for computational efficiency, we are able to reasonably reproduce previous results from both simple and more sophisticated models (Table 4).

Permafrost CO_2 emissions by 2100 in RCP8.5 fall within one standard deviation of the value found by Schuur et al. (2015), and within the range given by Koven et al. (2015b) (Table 4). The values given in Schuur et al. (2015) include the entire

https://doi.org/10.5194/gmd-2020-377
Preprint. Discussion started: 8 January 2021

Geoscientific Model Development Discussions

Table 4. Comparison of Hector's results to values from previous studies. Since Hector does not account for permafrost in terms of area, we estimated the values for comparison to McGuire et al. (2018) based on the fraction of permafrost lost over this time period, multiplied by the initial permafrost area in McGuire et al. (2018).

Scenario	Source	Variable	Value	Hector
RCP8.5	Burke et al. (2020)	Permafrost Remaining 2005-2100 (%)	37	33
RCP4.5	McGuire et al. (2018)	Permafrost Lost 2010-2299 (x10^6 km^2)	4.1	6.6
RCP8.5	McGuire et al. (2018)	Permafrost Lost 2010-2299 (x10^6 km^2)	12.7	12.1
RCP8.5	Schuur et al. (2015)	Cumulative Permafrost CO_2 Emissions 2010-2100 (Pg C)	92	110.5
RCP8.5	Koven et al. (2015)	Cumulative Permafrost CO_2 Emissions 2010-2100 (Pg C)	27.9-112.6	110.5
RCP8.5	Koven et al. (2015)	Permafrost CH_4 Flux Change 2010-2100 (Pg C yr^{-1})	3.97-10.48	26.8
RCP8.5	Crichton et al. (2016)	Permafrost-Driven Temperature Change by 2100	10-40%	10-30%

permafrost profile rather than 0-3m as is represented in our model, so this may imply our estimates are slightly higher in comparison.

Methane emissions were somewhat high in Hector compared to estimates by Koven et al. (2015b), though comparing an annual flux value makes it particularly sensitive to the timing of the peak so this difference may be driven by a somewhat later, or much earlier, peak in Hector's emissions. Even during the uncalibrated period of Hector, the land area of permafrost lost still aligns fairly closely with estimates from McGuire et al. (2018).

Previous estimates of the temperature amplification of permafrost carbon feedback by the end of the century cover a wide range, from 0.02 to 0.36°C in Burke et al. (2013); Schneider von Deimling et al. (2012) and Schneider von Deimling et al. (2015),from 0.1 to 0.8 °C in (MacDougall et al., 2012, 2013), from 10-40% of peak temperature change (Crichton et al., 2016), and 0.2 to 12% of peak temperature change in (Burke et al., 2017). In Hector, we find a temperature amplification due to permafrost emissions of 9-30%, or 0.4-0.5°C, by 2100 across all four RCPs (Table 3), which falls closely within the range of Crichton et al. (2016) but higher than the estimates in Burke et al. (2017).

4.3 Conclusions

The addition of permafrost thaw in Hector provides a useful tool for understanding the potential impact of the permafrost carbon feedback over the next decades and centuries, a particularly important capability in the context of ongoing climate change and uncertain impacts of permafrost thaw. The model's simplicity means that it can cheaply run uncertainty analyses over a wide range of parameter values to account for the remaining gaps in our knowledge of permafrost controls. In the future, Hector's permafrost module can be easily coupled with integrated assessment models like GCAM to estimate the economic consequences of warming from this feedback and to improve evaluation of climate and energy policy using such models.

https://doi.org/10.5194/gmd-2020-377
Preprint. Discussion started: 8 January 2021


Geoscientific Model Development Discussions
Open Access
EGU

5 Code availability

The version of Hector used in this analysis is available at https://github.com/dawnlwoodard/hector/tree/permafrost-submodel and the code used to generate the tables and figures is available at: https://github.com/dawnlwoodard/hector-permafrost-analysis.

Author contributions. A.N.S. developed an initial version of this model under the mentorship of C.H. D.L.W. updated and revised it to the current version under the mentorship of B.B.-L., as well as analyzed results and performed a sensitivity analysis. D.L.W. wrote the manuscript with contributions from all co-authors.

Competing interests. The authors declare that they have no conflict of interest.

Acknowledgements. The authors would like to thank Christina Schädel for her valuable feedback and suggestions on this research. This work was based on research supported by the U.S. Department of Energy (DOE), Office of Science, Biological and Environmental Research, as part of the Regional and Global Model Analysis program. This research is also supported in part by US Environmental Protection Agency, under Interagency Agreement DW-089-92459801. The views and opinions expressed are those of the authors and do not necessarily represent the views or policies of the US EPA or other funding organizations. Support for B.K. was provided in part by the National Science Foundation through agreement CBET-1931641, the Indiana University Environmental Resilience Institute, and the it Prepared for Environmental Change Grand Challenge initiative. The Pacific Northwest National Laboratory is operated for the US Department of Energy by Battelle Memorial Institute under contract DE-AC05-76RL01830. Support for A.N.S. was provided in part by the NASA Surface Biology and Geology (SBG) mission study.

https://doi.org/10.5194/gmd-2020-377
Preprint. Discussion started: 8 January 2021

Geoscientific Model Development Discussions
Open Access
EGU

References

Andresen, C. G., Lawrence, D. M., Wilson, C. J., McGuire, A. D., Koven, C., Schaefer, K., Jafarov, E., Peng, S., Chen, X., Gouttevin, I., et al.: Soil moisture and hydrology projections of the permafrost region–a model intercomparison, The Cryosphere (Online), 14, 2020.

Anthony, K. W., von Deimling, T. S., Nitze, I., Frolking, S., Emond, A., Daanen, R., Anthony, P., Lindgren, P., Jones, B., and Grosse, G.: 21st-century modeled permafrost carbon emissions accelerated by abrupt thaw beneath lakes, Nature communications, 9, 1–11, 2018.

Arango-Aramburo, S., Turner, S. W., Daenzer, K., Ríos-Ocampo, J. P., Hejazi, M. I., Kober, T., Álvarez-Espinosa, A. C., Romero-Otalora, G. D., and van der Zwaan, B.: Climate impacts on hydropower in Colombia: A multi-model assessment of power sector adaptation pathways, Energy policy, 128, 179–188, 2019.

Bond-Lamberty, B., Smith, A. P., and Bailey, V.: Temperature and moisture effects on greenhouse gas emissions from deep active-layer boreal soils, Biogeosciences, 13, 6669–6681, https://doi.org/10.5194/bg-13-6669-2016, 2016.

Burke, E. J., Hartley, I. P., and Jones, C. D.: Uncertainties in the global temperature change caused by carbon release from permafrost thawing, The Cryosphere, 6, 1063–1076, https://doi.org/10.5194/tc-6-1063-2012, 2012.

Burke, E. J., Jones, C. D., and Koven, C. D.: Estimating the permafrost-carbon climate response in the CMIP5 climate models using a simplified approach, Journal of Climate, 26, 4897–4909, https://doi.org/10.1175/jcli-d-12-00550.1, 2013.

Burke, E. J., Ekici, A., Huang, Y., Chadburn, S. E., Huntingford, C., Ciais, P., Friedlingstein, P., Peng, S., and Krinner, G.: Quantifying uncertainties of permafrost carbon-climate feedbacks, Biogeosciences Discussions, pp. 1–42, https://doi.org/10.5194/bg-2016-544, 2017.

Burke, E. J., Zhang, Y., and Krinner, G.: Evaluating permafrost physics in the Coupled Model Intercomparison Project 6 (CMIP6) models and their sensitivity to climate change, The Cryosphere, 14, 3155–3174, https://doi.org/10.5194/tc-14-3155-2020, 2020.

Chadburn, S., Burke, E., Essery, R., Boike, J., Langer, M., Heikenfeld, M., Cox, P., and Friedlingstein, P.: An improved representation of physical permafrost dynamics in the JULES land-surface model, Geoscientific Model Development, 8, 1493–1508, https://doi.org/10.5194/gmd-8-1493-2015, 2015.

Chadburn, S. E., Burke, E. J., Cox, P. M., Friedlingstein, P., Hugelius, G., and Westermann, S.: An observation-based constraint on permafrost loss as a function of global warming, Nature Climate Change, 7, 340–344, https://doi.org/10.1038/nclimate3262, 2017.

Chen, Y., Liu, A., Zhang, Z., Hope, C., and Crabbe, M. J. C.: Economic losses of carbon emissions from circum-Arctic permafrost regions under RCP-SSP scenarios, Science of The Total Environment, 658, 1064–1068, https://doi.org/10.1016/j.scitotenv.2018.12.299, 2019.

Clarke, L., Eom, J., Marten, E. H., Horowitz, R., Kyle, P., Link, R., Mignone, B. K., Mundra, A., and Zhou, Y.: Effects of long-term climate change on global building energy expenditures, Energy Economics, 72, 667–677, https://doi.org/10.1016/j.eneco.2018.01.003, 2018.

Crichton, K. A., Bouttes, N., Roche, D. M., Chappellaz, J., and Krinner, G.: Permafrost carbon as a missing link to explain CO_2 changes during the last deglaciation, Nature Geoscience, 9, 683–686, https://doi.org/10.1038/ngeo2793, 2016.

Elberling, B., Michelsen, A., Schädel, C., Schuur, E. A. G., Christiansen, H. H., Berg, L., Tamstorf, M. P., and Sigsgaard, C.: Long-term CO_2 production following permafrost thaw, Nature Climate Change, 3, 890–894, https://doi.org/10.1038/nclimate1955, 2013.

Frost, G. V. and Epstein, H. E.: Tall shrub and tree expansion in Siberian tundra ecotones since the 1960s, Global Change Biology, 20, 1264–1277, https://doi.org/10.1111/gcb.12406, 2014.

Gruber, S.: Derivation and analysis of a high-resolution estimate of global permafrost zonation, The Cryosphere, 6, 221–233, https://doi.org/10.5194/tc-6-221-2012, 2012.

https://doi.org/10.5194/gmd-2020-377
Preprint. Discussion started: 8 January 2021

Geoscientific Model Development Discussions

Hartin, C. A., Patel, P., Schwarber, A., Link, R. P., and Bond-Lamberty, B. P.: A simple object-oriented and open-source model for scientific and policy analyses of the global climate system – Hector v1.0, Geoscientific Model Development, 8, 939–955, https://doi.org/10.5194/gmd-8-939-2015, 2015.

Hartin, C. A., Bond-Lamberty, B., Patel, P., and Mundra, A.: Ocean acidification over the next three centuries using a simple global climate carbon-cycle model: projections and sensitivities, Biogeosciences, 13, 4329–4342, https://doi.org/10.5194/bg-13-4329-2016, 2016.

Hope, C. and Schaefer, K.: Economic impacts of carbon dioxide and methane released from thawing permafrost, Nature Climate Change, 6, 56–59, https://doi.org/10.1038/nclimate2807, 2015.

Hugelius, G., Strauss, J., Zubrzycki, S., Harden, J. W., Schuur, E. A. G., Ping, C.-L., Schirrmeister, L., Grosse, G., Michaelson, G. J., Koven, C. D., and al., e.: Estimated stocks of circumpolar permafrost carbon with quantified uncertainty ranges and identified data gaps, Biogeosciences, 11, 6573–6593, https://doi.org/10.5194/bg-11-6573-2014, 2014.

Kessler, L.: Estimating the economic impact of the permafrost carbon feedback, Climate Change Economics, 8, 1750 008, https://doi.org/10.1142/s2010007817500087, 2017.

Knoblauch, C., Beer, C., Liebner, S., Grigoriev, M. N., and Pfeiffer, E.-M.: Methane production as key to the greenhouse gas budget of thawing permafrost, Nature Climate Change, 8, 309–312, https://doi.org/10.1038/s41558-018-0095-z, 2018.

Koven, C. D., Ringeval, B., Friedlingstein, P., Ciais, P., Cadule, P., Khvorostyanov, D., Krinner, G., and Tarnocai, C.: Permafrost carbon-climate feedbacks accelerate global warming, Proceedings of the National Academy of Sciences, 108, 14 769–14 774, https://doi.org/10.1073/pnas.1103910108, 2011.

Koven, C. D., Riley, W. J., and Stern, A.: Analysis of permafrost thermal dynamics and response to climate change in the CMIP5 earth system models, Journal of Climate, 26, 1877–1900, https://doi.org/10.1175/jcli-d-12-00228.1, 2013.

Koven, C. D., Lawrence, D. M., and Riley, W. J.: Permafrost carbon-climate feedback is sensitive to deep soil carbon decomposability but not deep soil nitrogen dynamics, Proceedings of the National Academy of Sciences, p. 201415123, https://doi.org/10.1073/pnas.1415123112, 2015a.

Koven, C. D., Schuur, E. A. G., Schädel, C., Bohn, T. J., Burke, E. J., Chen, G., Chen, X., Ciais, P., Grosse, G., Harden, J. W., and al., e.: A simplified, data-constrained approach to estimate the permafrost carbon-climate feedback, Philosophical Transactions of the Royal Society A: Mathematical, Physical and Engineering Sciences, 373, 20140 423, https://doi.org/10.1098/rsta.2014.0423, 2015b.

Lawrence, D. M., Slater, A. G., and Swenson, S. C.: Simulation of present-day and future permafrost and seasonally frozen ground conditions in CCSM4, Journal of Climate, 25, 2207–2225, https://doi.org/10.1175/jcli-d-11-00334.1, 2012.

Lawrence, D. M., Koven, C. D., Swenson, S. C., Riley, W. J., and Slater, A.: Permafrost thaw and resulting soil moisture changes regulate projected high-latitude CO_2 and CH_4 emissions, Environmental Research Letters, 10, 094 011, https://doi.org/10.1088/1748-9326/10/9/094011, 2015.

LeBauer, D. S., Wang, D., Richter, K. T., Davidson, C. C., and Dietze, M. C.: Facilitating feedbacks between field measurements and ecosystem models, Ecological Monographs, 83, 133–154, https://doi.org/10.1890/12-0137.1, 2013.

MacDougall, A. H., Avis, C. A., and Weaver, A. J.: Significant contribution to climate warming from the permafrost carbon feedback, Nature Geoscience, 5, 719–721, https://doi.org/10.1038/ngeo1573, 2012.

MacDougall, A. H., Eby, M., and Weaver, A. J.: If anthropogenic CO_2 emissions cease, will atmospheric CO_2 concentration continue to increase?, Journal of climate, 26, 9563–9576, https://doi.org/10.1175/JCLI-D-12-00751.1, 2013.

Matveev, A., Laurion, I., Deshpande, B. N., Bhiry, N., and Vincent, W. F.: High methane emissions from thermokarst lakes in subarctic peatlands, Limnology and Oceanography, 61, S150–S164, https://doi.org/10.1002/lno.10311, 2016.

https://doi.org/10.5194/gmd-2020-377
Preprint. Discussion started: 8 January 2021

McGuire, A. D., Lawrence, D. M., Koven, C., Clein, J. S., Burke, E., Chen, G., Jafarov, E., MacDougall, A. H., Marchenko, S., Nicolsky, D., et al.: Dependence of the evolution of carbon dynamics in the northern permafrost region on the trajectory of climate change, Proceedings of the National Academy of Sciences, 115, 3882–3887, https://doi.org/10.1073/pnas.1719903115, 2018.

Meinshausen, M., Raper, S. C. B., and Wigley, T. M. L.: Emulating coupled atmosphere-ocean and carbon cycle models with a simpler model, MAGICC6 – Part 1: Model description and calibration, Atmospheric Chemistry and Physics, 11, 1417–1456, https://doi.org/10.5194/acp-11-1417-2011, 2011.

Moss, R. H., Edmonds, J. A., Hibbard, K. A., Manning, M. R., Rose, S. K., Van Vuuren, D. P., Carter, T. R., Emori, S., Kainuma, M., Kram, T., et al.: The next generation of scenarios for climate change research and assessment, Nature, 463, 747–756, https://doi.org/10.1038/nature08823, 2010.

Pithan, F. and Mauritsen, T.: Arctic amplification dominated by temperature feedbacks in contemporary climate models, Nature Geoscience, 7, 181–184, https://doi.org/10.1038/ngeo2071, 2014.

Pörtner, H., Roberts, D., Masson-Delmotte, V., Zhai, P., Tignor, M., Poloczanska, E., Mintenbeck, K., Nicolai, M., Okem, A., Petzold, J., et al.: IPCC Special Report on the Ocean and Cryosphere in a Changing Climate, IPCC Intergovernmental Panel on Climate Change: Geneva, Switzerland, 2019.

Romanovsky, V. E., Smith, S. L., and Christiansen, H. H.: Permafrost thermal state in the polar Northern Hemisphere during the international polar year 2007–2009: a synthesis, Permafrost and Periglacial Processes, 21, 106–116, https://doi.org/10.1002/ppp.689, 2010.

Schädel, C., Schuur, E. A. G., Bracho, R., Elberling, B., Knoblauch, C., Lee, H., Luo, Y., Shaver, G. R., and Turetsky, M. R.: Circumpolar assessment of permafrost C quality and its vulnerability over time using long-term incubation data, Global Change Biology, 20, 641–652, https://doi.org/10.1111/gcb.12417, 2014.

Schädel, C., Bader, M. K.-F., Schuur, E. A., Biasi, C., Bracho, R., Čapek, P., De Baets, S., Diáková, K., Ernakovich, J., Estop-Aragones, C., et al.: Potential carbon emissions dominated by carbon dioxide from thawed permafrost soils, Nature Climate Change, 6, 950–953, https://doi.org/10.1038/nclimate3054, 2016.

Schneider von Deimling, T., Meinshausen, M., Levermann, A., Huber, V., Frieler, K., Lawrence, D. M., and Brovkin, V.: Estimating the near-surface permafrost-carbon feedback on global warming, Biogeosciences, 9, 649–665, https://doi.org/10.5194/bg-9-649-2012, 2012.

Schneider von Deimling, T., Grosse, G., Strauss, J., Schirrmeister, L., Morgenstern, A., Schaphoff, S., Meinshausen, M., and Boike, J.: Observation-based modelling of permafrost carbon fluxes with accounting for deep carbon deposits and thermokarst activity, Biogeosciences, 12, 3469–3488, https://doi.org/10.5194/bg-12-3469-2015, 2015.

Schuur, E., McGuire, A., Romanovsky, V., Schädel, C., and Mack, M.: Chapter 11: Arctic and boreal carbon, Second State of the Carbon Cycle Report (SOCCR2): A sustained assessment report, pp. 428–468, 2018.

Schuur, E. A., Abbott, B., Bowden, W., Brovkin, V., Camill, P., Canadell, J., Chanton, J., Chapin, F., Christensen, T., Ciais, P., et al.: Expert assessment of vulnerability of permafrost carbon to climate change, Climatic Change, 119, 359–374, https://doi.org/10.1007/s10584-013-0730-7, 2013.

Schuur, E. A. G., McGuire, A. D., Schädel, C., Grosse, G., Harden, J. W., Hayes, D. J., Hugelius, G., Koven, C. D., Kuhry, P., Lawrence, D. M., and al., e.: Climate change and the permafrost carbon feedback, Nature, 520, 171–179, https://doi.org/10.1038/nature14338, 2015.

Shur, Y. L. and Jorgenson, M.: Patterns of permafrost formation and degradation in relation to climate and ecosystems, Permafrost and Periglacial Processes, 18, 7–19, https://doi.org/10.1002/ppp.582, 2007.

https://doi.org/10.5194/gmd-2020-377
Preprint. Discussion started: 8 January 2021

Stocker, T. F., Qin, D., Plattner, G.-K., Tignor, M., Allen, S. K., Boschung, J., Nauels, A., Xia, Y., Bex, V., Midgley, P. M., et al.: Climate change 2013: The physical science basis, Contribution of working group I to the fifth assessment report of the intergovernmental panel on climate change, 1535, 2013.

Treat, C. C., Wollheim, W. M., Varner, R. K., Grandy, A. S., Talbot, J., and Frolking, S.: Temperature and peat type control CO_2 and CH_4 production in Alaskan permafrost peats, Global Change Biology, 20, 2674–2686, https://doi.org/10.1111/gcb.12572, 2014.

Turetsky, M. R., Wieder, R., and Vitt, D. H.: Boreal peatland C fluxes under varying permafrost regimes, Soil Biology and Biochemistry, 34, 907–912, https://doi.org/10.1016/s0038-0717(02)00022-6, 2002.

Turetsky, M. R., Abbott, B. W., Jones, M. C., Anthony, K. W., Olefeldt, D., Schuur, E. A., Grosse, G., Kuhry, P., Hugelius, G., Koven, C., et al.: Carbon release through abrupt permafrost thaw, Nature Geoscience, 13, 138–143, https://doi.org/10.1038/s41561-019-0526-0, 2020.

Vega-Westhoff, B., Sriver, R. L., Hartin, C. A., Wong, T. E., and Keller, K.: Impacts of observational constraints related to sea level on estimates of climate sensitivity, Earth's Future, 7, 677–690, 2019.

Vonk, J. E., Tank, S. E., Bowden, W. B., Laurion, I., Vincent, W. F., Alekseychik, P., Amyot, M., Billet, M., Canario, J., Cory, R. M., et al.: Reviews and syntheses: Effects of permafrost thaw on Arctic aquatic ecosystems, Biogeosciences, 12, 7129–7167, https://doi.org/10.5194/bg-12-7129-2015, 2015.

Wickland, K. P., Striegl, R. G., Neff, J. C., and Sachs, T.: Effects of permafrost melting on CO_2 and CH_4 exchange of a poorly drained black spruce lowland, Journal of Geophysical Research: Biogeosciences, 111, n/a–n/a, https://doi.org/10.1029/2005jg000099, 2006.

Yumashev, D., Hope, C., Schaefer, K., Riemann-Campe, K., Iglesias-Suarez, F., Jafarov, E., Burke, E. J., Young, P. J., Elshorbany, Y., and Whiteman, G.: Climate policy implications of nonlinear decline of Arctic land permafrost and other cryosphere elements, Nature Communications, 10, 1–11, https://doi.org/10.1038/s41467-019-09863-x, 2019.